

Mechanism of the $^{22}\text{Ne}(d,^6\text{Li})^{18}\text{O}$ reaction

W. Oelert, G. Pálla,* B. Rubio, M. G. Betigeri,† C. Mayer-Böricke, and P. Turek
Institut für Kernphysik, Kernforschungsanlage Jülich, D-5170 Jülich, Federal Republic of Germany

H. T. Fortune

Physics Department, University of Pennsylvania, Philadelphia, Pennsylvania 19104

(Received 22 May 1984)

As part of a systematic study, the $(d,^6\text{Li})$ reaction has been measured at a bombarding energy of 80 MeV on ^{22}Ne . Angular distributions were obtained in an angular range of 8° to 35° (lab). In the framework of finite-range distorted-wave Born approximation calculations, alpha spectroscopic factors were extracted. The strong collectivity of the low-lying states suggests the necessity of employing a coupled reaction channels formalism in the analysis. Indeed spectroscopic information arising from one-channel distorted-wave Born approximation calculations reveals significant differences between experimental and theoretical results. Furthermore, the shapes of some experimental angular distributions are not fitted by the distorted-wave Born approximation method. Both give indications of an insufficiency of the simple one-channel calculations—at least for strong collective states.

I. INTRODUCTION

An investigation on the structure of low-lying positive-parity states in ^{18}O (Ref. 1) resulted in the conclusion that the major components of the wave function for all positive-parity states below 7.2 MeV ($> 95\%$ in all cases) arise from the $(0d_{5/2}, 1s_{1/2})$ model space plus one core-excited collective state of each of the spins 0^+ , 2^+ , and 4^+ . These collective states are roughly the second 0^+ state at 3.63 MeV, the third 2^+ state at 5.25 MeV, and the second 4^+ state at 7.11 MeV excitation energy. Based on those results one might expect that the properties of the pickup strengths in the transfer reaction $^{22}\text{Ne}(d,^6\text{Li})^{18}\text{O}$ to most of the low-lying levels should be well described by calculations of alpha spectroscopic factors² from complete $d_{5/2}$ - $s_{1/2}$ - $d_{3/2}$ shell-model wave functions as generated by the Chung-Wildenthal interaction.³ In order to test this hypothesis, the alpha-transfer reaction leading to final states in ^{18}O has been measured at a deuteron energy of 80 MeV.

In a first step the analysis was performed in the exact finite-range distorted-wave Born approximation (FR-DWBA). The results are discussed and compared to shell-model predictions.² The lack of agreement between experimental and theoretical results suggests the need for coupled channel calculations. The necessity of taking this complicated reaction mechanism into account is investigated by coupled reaction channel (CRC) and coupled-channel distorted-wave (CCDW) calculations.

II. EXPERIMENTAL PROCEDURE

The 80-MeV deuteron beam from the Jülich Isochronous Cyclotron JULIC was used to measure angular distributions of the $^{22}\text{Ne}(d,^6\text{Li})^{18}\text{O}$ reaction in the angular range of 8° to 35° laboratory. An excitation energy range up to 30 MeV was covered, but states excited with significant strength were observed only up to 10 MeV excitation

energy. The experiment was performed using conventional ΔE - E surface barrier detector techniques. Two telescopes were used during the experiment; the thickness of the ΔE and E detectors was 100 and 1000 μm , respectively. The particle identification was sufficient to ensure separation between the outgoing ^6Li and ^7Li ions. A gas cell filled at a pressure of 300 Torr at 25°C (corresponding to an equivalent target thickness of 0.8 mg/cm^2 at 20° reaction angle for the present setup) with Ne gas isotopically enriched to 95.3% of ^{22}Ne was used as the target. Counts arising from impurities, mainly ^{20}Ne , are observable in the energy spectra but have no significant influence on the low-lying states. A typical spectrum of the $^{22}\text{Ne}(d,^6\text{Li})^{18}\text{O}$ reaction, taken at $\theta_{\text{lab}} = 15.0^\circ$, is shown in Fig. 1. Only an excitation energy range up to 11 MeV is displayed as no significant peaks were observed at higher excitation energies. Seven peaks have been clearly identified and were analyzed, at least one of which (peak No. 7, at excitation energy of about 9.4 MeV) appears to be an unresolved doublet. The incident beam current was continuously monitored by a Ge(Li) detector at an angle of 30° laboratory relative to the beam direction. The ratio of the deuteron yield elastically scattered into the monitor counter to the integrated charge collected in a Faraday cup was used to ensure the accuracy of the determination

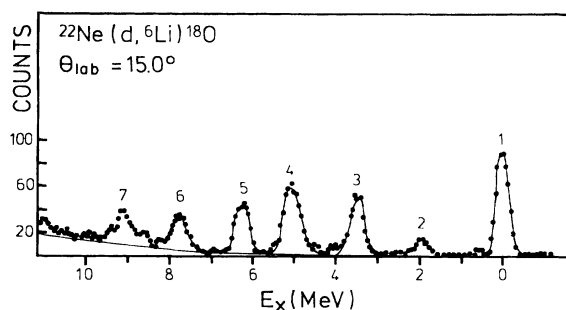


FIG. 1. Energy spectrum of the $^{22}\text{Ne}(d,^6\text{Li})^{18}\text{O}$ reaction.

of the relative cross sections at the various angles; this ratio was always constant within 5%. The absolute cross sections were determined by the integrated charge only and are believed to be accurate within 20%, as long as this uncertainty is less than the errors arising from counting statistics.

Because of the rather small cross sections, it was necessary to use a high intensity achromatic beam, ranging from 10 nA to 1.3 μA on the target, depending on the reaction angle. In addition to the energy spread of the beam itself, contributions from the target thickness, gas cell walls, and angular acceptance of the detectors resulted in an overall energy resolution of typically 350 keV full width at half maximum (FWHM).

III. EXTRACTION OF SPECTROSCOPIC FACTORS BY DWBA ANALYSIS

The experimental angular distributions were compared to finite-range DWBA calculations to extract alpha spectroscopic factors. The DWBA code LOLA (Ref. 4) was employed in the "post" representation assuming an alpha-cluster transfer. Parameters for the bound state wave function of the alpha cluster (in the target nucleus and in the outgoing ^6Li particle) were chosen as described earlier.⁵ The deuteron optical-model potential was selected basically according to Ref. 6; however, the spin-orbit part of the potential was neglected. Further details on the choice of the parameters are presented elsewhere.⁷ For the ^6Li optical-model potentials, the parameters are basically those of Chua *et al.*;⁸ the depth of the real well was adjusted to fit the experimental ground-state transfer $^{22}\text{Ne}(d, ^6\text{Li})^{18}\text{O}$ angular distribution.

A DWBA calculation using a ^6Li potential depth of $V_R = 203$ MeV for the real volume part [close to the value of $V_R = 210$ MeV used before⁵ for the $^{20}\text{Ne}(d, ^6\text{Li})^{16}\text{O}$ reaction] fits the data very well as can be seen in Fig. 2 by the dashed line. However, as argued earlier⁷ and based on the systematic study by Lezoch *et al.*,⁹ a real potential depth of 153 MeV for the ^6Li optical potential seems to be more physical. This smaller potential depth leads to the same quality of fit between DWBA prediction and experimental angular distribution shape for the ground-state transition, as demonstrated by the solid line in Fig. 2. Qualitatively the same result is observed for the excited states and, furthermore, the relative spectroscopic factors extracted for final states in ^{18}O (relative to the ground-state transition) are identical within 8% using either of the potential depths. Figures 3 and 4 show experimental angular distributions for final states in ^{18}O which are rather strongly excited in the $(d, ^6\text{Li})$ reaction on ^{22}Ne . The experimental ground-state spectroscopic factor [relative to the $^{20}\text{Ne}(d, ^6\text{Li})^{16}\text{O}$ g.s. transition] increases insignificantly from 0.25 to 0.29 for the ^6Li potential depths of 203 and 153 MeV, respectively, compared to the predicted theoretical values of 0.55 and 0.34, resulting from shell-model² and SU(3) (Ref. 10) calculations, respectively. The optical-model parameters used in the final analysis are given in Table I.

Table II summarizes the results obtained in the present investigation, compared to values given in the literature¹¹

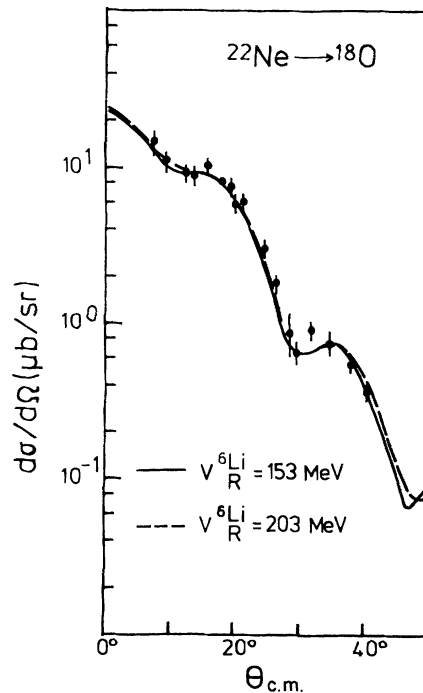


FIG. 2. Ground state transition angular distribution compared to FR-DWBA calculations using different ^6Li optical potential depths. Only statistical errors are included in the data.

and predicted by shell-model calculations.³ It is interesting to note that the shell-model calculations, which were done in the full $d_{5/2}$, $s_{1/2}$, and $d_{3/2}$ model space, predict no state in ^{18}O between 4.03 and 8.21 MeV excitation energy except for the unnatural-parity 3^+ state at 5.529 MeV. The structures of states in this excitation energy range obviously involve hole contributions from the lower $1p$ shell of the ^{16}O core.

It is seen from Fig. 1 that the $(d, ^6\text{Li})$ reaction excites

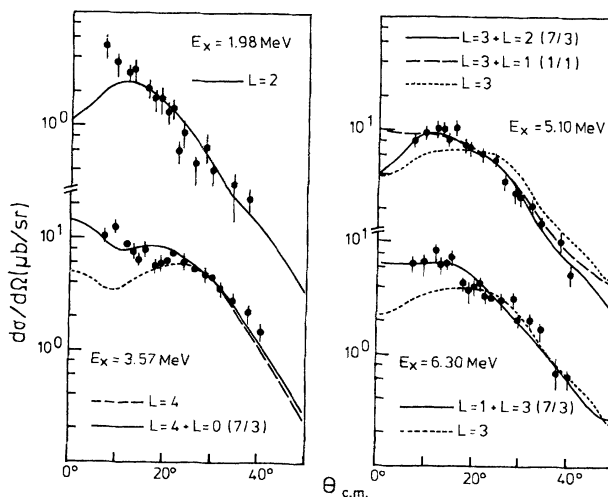


FIG. 3. Experimental angular distributions for the $^{22}\text{Ne}(d, ^6\text{Li})^{18}\text{O}$ reaction compared to FR-DWBA calculations. Only statistical errors are included in the data.

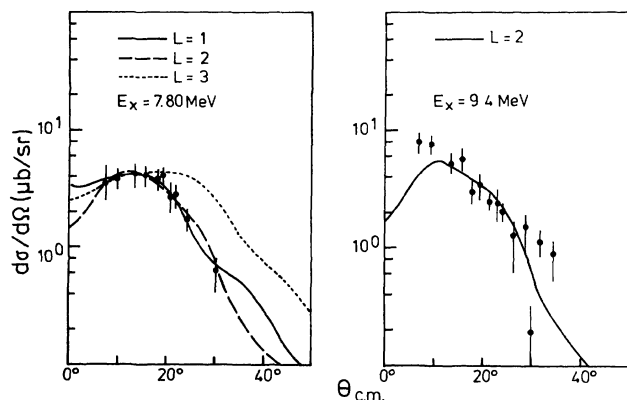


FIG. 4. Experimental angular distributions for the $^{22}\text{Ne}(d,^6\text{Li})^{18}\text{O}$ reaction compared to FR-DWBA calculations. Only statistical errors are included in the data.

selectively six peaks up to an excitation energy of 8 MeV. This is qualitatively in agreement with the same type of data measured with high resolution at $E_d = 55$ MeV.¹²

IV. DISCUSSION OF THE RESULTS IN THE DWBA FORMALISM

The extraction of spectroscopic factors employing the DWBA formalism presumes the validity of a one-step direct reaction mechanism. Furthermore, in the cases of experimentally unresolved higher excited levels it is assumed that each of the incoherently combined DWBA curves would fit the corresponding angular distribution for the individual state, an assumption which has been used frequently in the literature; see, e.g., Ref. 7.

The ground state (peak 1) and the first excited state (peak 2) are supposed to consist of wave functions mainly represented by $d_{5/2}$ and $s_{1/2}$ components.¹ Shell-model calculations from complete $d_{5/2}$ - $s_{1/2}$ - $d_{3/2}$ wave functions are expected to predict the spectroscopic information reasonably well; and in fact, within a factor of 2, experimental and theoretical relative spectroscopic factors agree with each other. In view of the estimated experimental error (20%), however, this factor of 2 is significant and

too large to be ignored. The experimental angular distributions are rather well described by FR-DWBA calculations, except that for the 2^+ final state some disagreement is observed for angles smaller than 15° .

The present experimental setup does not resolve the two states known within the excitation energy range of peak 3 in Fig. 1 (4^+ at 3.555 MeV and $0_2^+ = 3.634$ MeV). The angular distribution of this peak ($E_x = 3.57$ MeV) is shown in Fig. 3 and indicates a dominant angular momentum transfer of $L=4$. However, a reasonable fit to the data is achieved only if an $L=0$ contribution is also taken into account (the solid line in Fig. 3 for $E_x = 3.57$ MeV is an incoherent summation of 70% for $L=4$ and 30% for $L=0$ FR-DWBA predicted strength). The extracted spectroscopic factors are given in Table II in the limits of no $L=0$ and 30% of DWBA predicted $L=0$ strengths, leading to a 0^+ relative spectroscopic factor between 0 and 0.27. Even the spectrum of the high resolution experiment¹² does not clearly resolve both final states. However, it again indicates that the strength of this 0_2^+ state should be less than about 20% of the ground-state transition strength. The shell model, on the other hand, predicts a relative spectroscopic factor (0.05 relative to the ground-state transition) which is so small that its excitation would be barely observable in the present experiment. The apparent disagreement between the experimental result and the shell-model calculation³ for this 0^+ state is understood as being due to the limited shell-model space. According to Ref. 1, 75% of the wave function for the 0_2^+ state is due to core excited components,¹ the sum of the $(d_{5/2})_0^2$ and $(s_{1/2})_0^2$ intensities being only 0.25. In this sense the agreement between experiment and prediction³ is, in fact, rather good since in lowest order only a small fraction of the experimentally observed strength is expected to be predictable by the $(sd)^2$ shell model. The upper limit of the relative experimental spectroscopic factor has been determined to be 0.27 (see Table I and discussion above), which would lead to an upper limit of the relative spectroscopic factor due to sd -shell components of only 0.07, in good agreement with the predicted value of 0.05.

The experimentally known¹² 2_2^+ state at 3.92 MeV excitation energy has, according to the shell-model calculation (4.034 MeV), a small spectroscopic factor (0.02 relative to the ground state, i.e., $\frac{1}{3}$ of the strength of the first excited 2_1^+ state). Qualitatively this result is in agreement with

TABLE I. Optical model potential parameters^a used in the analysis (potential strengths in MeV, lengths in fm).

Particles	V_R	r_R	a_R	W_I	r_I	a_I	W_D	r_D	a_D	r_c
$d + ^{22}\text{Ne}$	-74.76	1.25 ^{b,c}	0.79	-3.969	1.33 ^b	0.677	9.62	1.33 ^b	0.677	1.30 ^b
$^6\text{Li} + ^{18}\text{O}$	-153.0	1.30 ^b	0.70	-12.4	1.70 ^b	0.90				1.40 ^b
Bound states	d	0.97 ^{c,f}	0.65							

^aThe analytical expression of the optical potential is

$$V = V_c + V_R f(r, R_R, a_R) + iW_I f(r, R_I, a_I) + iW_D 4a_D [d/dr f(r, R_D, a_D)] \text{ with } f(r, R_N, a_N) = \{1 + \exp[(r - R_N)/a_N]\}^{-1}.$$

^b $R_N = r_N A^{1/3}$, $N = R, I, D$.

^c $R_R = r_R (A^{1/3} + 4^{1/3})$, $N = R, I, D$.

^dPotential depths of the bound states for the systems " α particle in target" and " α particle in ^6Li " adjusted to fit the α -particle separation energies.

^eFor the ZR calculations the value of 1.15 was used; see Ref. 6.

^fFor the ZR calculations a bound state radius parameter of 1.00 fm was used.

TABLE II. Results of the FR analysis of the $^{22}\text{Ne}(d,^6\text{Li})^{18}\text{O}$ reaction.

E_x (MeV) Ref. 11	J^π	Peak No. in Fig. 1	Present		Shell model		
			E_x^d (MeV)	S_α^{rel}	E_x (MeV)	J^π Ref. 3	S_α^{rel}
0.000	0 ⁺	1	0.00	1(0.27) ^c	0.000	0 ⁺	1(0.55) ^c
1.982	2 ⁺	2	1.98	0.16	2.000	2 ⁺	0.07
3.555	4 ⁺	3	3.57	0.64→0.57 ^b	3.519	4 ⁺	0.84
3.634	0 ⁺			0.0→0.27	4.016	0 ⁺	0.05
3.920	2 ⁺		3.9	<0.04	4.034	2 ⁺	0.02
4.456	1 ⁻						
5.098	3 ⁻	4	5.10	0.91			
5.260	2 ⁺			0.40			
5.336	0 ⁺						
5.378	3 ⁺				5.529	3 ⁺	
5.530	2 ⁻						
6.198	1 ⁻	5	6.30	0.52			
6.351	(2 ⁻)						
6.404	3 ⁻						
6.880	0 ⁻			0.39			
7.117	4 ⁺						
7.618	1 ⁻						
7.77	2 ⁻						
7.860	(4 ⁺)	6	7.8	a			
7.977	(3 ⁺ ,4 ⁻)						
8.038	1 ⁻						
8.126	5 ⁻						
8.216	2 ⁺						
8.287	3 ⁻						
Many more levels		7	9.4	>0.18 ^c	8.209	4 ⁺	0.03
					9.446	1 ⁺	
					9.449	2 ⁺	0.08
					9.514	3 ⁺	
					10.101	1 ⁺	
					10.253	2 ⁺	0.01
	14.384	0 ⁺	<0.01				
	14.486	2 ⁺	<0.01				

^aSee text for discussion.

^bThe actual value depends on the spectroscopic factor of the not resolved 0⁺ state; see the text.

^cAssuming $Q=7$; i.e., this is the lower limit; see the text.

^dUncertainties in the measured excitation energies are estimated to be 40 keV for $E_x \leq 6$ MeV, or else 100 keV.

^eSpectroscopic factors relative to the $^{20}\text{Ne} \rightarrow ^{16}\text{O}(\text{g.s.})$ transition in parentheses, otherwise relative to the $^{22}\text{Ne} \rightarrow ^{18}\text{O}(\text{g.s.})$ transition.

the present data and with the high resolution spectrum of Ref. 12. Since this level is close to peak 3, has a low yield, and is superimposed on some background, its yield has been extracted at only a few angles. From these limited data, the estimated relative spectroscopic factor is less than 0.04, and therefore in the sense of being small it can be regarded as being in good agreement with the shell-model prediction (0.02). The wave function of this 2_2^+ state is supposed¹ to consist of 75% of $(d_{5/2})_2^2$ and $(d_{5/2}, s_{1/2})_2$ contribution.

The peak observed at 5.10 MeV (No. 4) excitation energy is probably due mainly to the excitation of the known¹¹ 3^- state at 5.098 MeV. The FR-DWBA prediction, however, fits the angular distribution data, as seen in Fig. 3, only if a certain fraction of $L < 3$ transfer strength is included. Since from the energy scale and energy resolution point of view the 1^- state at 4.456 MeV is excluded, we

conclude that the states of this peak are excited by $L=2$ and 3 transfer strength leading to the final states 2_3^+ and 3_1^- . The relative spectroscopic factor extracted this way for the 2_3^+ state is 0.40 (see Table II). The spectrum of Ref. 12 indicates that this has to be considered as an upper limit and that a value of at least a factor of 3 smaller might be more realistic. In this case the FR-DWBA fit would be rather poor, as shown for the limit of no $L=2$ strength by the dotted line in Fig. 3.

The angular distribution of peak 5 (Fig. 3) with an excitation energy centered at 6.30 MeV seems well described by an incoherent sum of $L=1$ plus $L=3$ angular momentum transfer. In the $(d,^6\text{Li})$ experiment at 55 MeV (Ref. 12) the strength at this excitation energy range seems to be dominated by the yield for populating the 3^- state at 6.4 MeV, but the present angular distribution seems to include considerable $L=1$ strength due to the

known¹¹ 6.2 MeV 1^- state. The negative-parity states in ^{18}O consist of at least one hole in the p shell and therefore the spectroscopic factors are calculated with the quantum number for the relative motion

$$Q = 2N + L = \sum_{i=1}^4 (2n_i + l_i) = 7.$$

If these states were to consist mainly of three holes in the ^{16}O core ($Q = 5$), the spectroscopic factors given in Table I for negative-parity states would increase by a factor of up to 4. In that sense the values given for these states are regarded as lower limits.

At excitation energies of 7.8 and 9.4 MeV two peaks are observed, which very likely (i) involve more than the yield of one single final state, and (ii) reveal core excited nuclear structure. The compilation¹¹ lists several states near 7.8 MeV, including one with $J^\pi = 1^-$ at 7.618 MeV. States at 7.86 and 7.977 MeV have uncertain J^π , but the latter is probably of unnatural parity (3^+ or 4^-). An $L = 1$ curve gives an adequate account of the data, but $L = 2$ cannot be ruled out, whereas higher L transfers seem to be inadequate. Investigations¹³ of ^{18}O by the $^{12}\text{C}(^{18}\text{O}, ^{12}\text{C})^{18}\text{O}$ reaction suggest a state at 7.8 MeV with a spin-parity assignment of 2^+ , which is interpreted as having a 6p-4h configuration. The relative spectroscopic factor extracted in the present work would be 0.2 (1.3) [15] considering this state to be of pure 2p-0h (4p-2h) [6p-4h] nature. Since the angular distribution shape is not sensitive to the number of particle-hole configurations, the structure of this level cannot be decided in the present investigation.

Figure 4 displays also the angular distribution of the 9.4 MeV peak. An $L = 2$ transfer is consistent with the data; lower L values, however, cannot be excluded. Tentatively, $L = 2$ is assigned; the spectroscopic factor given in Table II indicates the lower limit, since likely particle-hole contributions were not included.

Figure 5 compares extracted α spectroscopic factors for the lowest 0^+ , 2^+ , and 4^+ levels with those calculated in the shell model, both being normalized to 1.0 for the g.s. Firstly, relative to S_α for $^{20}\text{Ne} \rightarrow ^{16}\text{O}(\text{g.s.})$, the experimental S_α for $^{22}\text{Ne} \rightarrow ^{18}\text{O}(\text{g.s.})$ is only 0.27 (Table II), whereas in the shell model this ratio is 0.55. Since the absolute

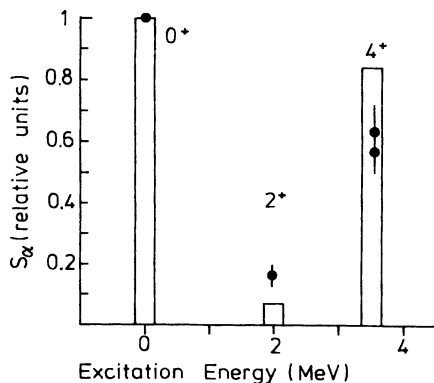


FIG. 5. Relative spectroscopic factors for the members of the ground state band in ^{18}O . The full points (solid lines) denote experimental (theoretical) spectroscopic factors relative to the ground state transitions.

cross sections are believed to be accurate to 20%, the factor of 2 discrepancy between relative experimental and theoretical results seems to be significant. It may be that the ^{18}O spectroscopic factor is too small or perhaps that for ^{16}O is too large, having been enhanced through core-excited components in $^{16}\text{O}(\text{g.s.})$, which are larger than in $^{18}\text{O}(\text{g.s.})$.

Relative to $S_\alpha(^{18}\text{O}(\text{g.s.}))$, the experimental value of $S_\alpha(2_1^+)$ is slightly larger than predicted, whereas that for $S_\alpha(4_1^+)$ is somewhat smaller than the shell-model value. We do note, however, that both the experimental and theoretical spectroscopic factors are quite small for 2_1^+ . The small cross section for the 1.98 MeV state and the failure to fit its angular distribution lead us to consider other reaction mechanisms, which we now discuss.

V. HIGHER ORDER PROCESSES

In view of the rather strong deformation of ^{22}Ne and ^{18}O we investigate the importance of coupling of the reaction channels. In this analysis, attention is restricted to the 0^+ , 2^+ , and 4^+ states. The coupling scheme used for the calculations is shown in Fig. 6. Transitions from ^{22}Ne to ^{18}O are preceded or followed by inelastic excitations. Reorientation effects¹⁴ with $L = 2$ are taken into account for the 2^+ state in either nucleus.

Spectroscopic amplitudes for transitions from the members of the ground state band in the target nucleus to final states in the residual nucleus were calculated using the shell model code of Chung *et al.*;³ the results are presented in Table III. The numbers listed are the spectroscopic factors relative to that for the ground-state to ground-state transition with the phases of the spectroscopic amplitudes for final states in ^{18}O , ordered by the individual angular momentum transfer (L). In the CRC calculations described below only a subset of the values given in Table III is used (see Fig. 6), viz., the spectroscopic factors and phases of the spectroscopic amplitudes leading from the 0_1^+ and 2_1^+ states in ^{22}Ne to the final states 0_1^+ , 2_1^+ , and 4_1^+ in ^{18}O ; the other numbers are given for completeness.

An inspection of Table III indicates that, e.g., the 2_1^+ final state in ^{18}O has a small relative spectroscopic factor (0.068) for the direct one-step transition, whereas the spectroscopic factor for the direct transition to the 4_1^+ state (0.842) is nearly as large as the ground state transition (1.0). This theoretical result already suggests that routes other than the direct one-step path may play important roles in exciting the 2_1^+ state (e.g., via the ground state

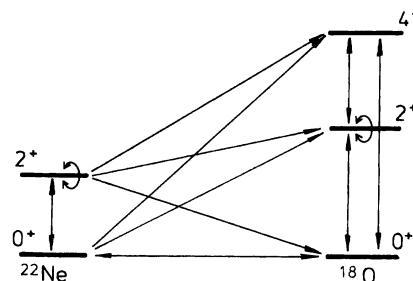


FIG. 6. Coupling scheme used for the CRC calculations.

TABLE III. Sign of spectroscopic amplitudes and spectroscopic factors for the transition $^{22}\text{Ne} \rightarrow ^{18}\text{O}$.

Final states ^{18}O		Initial states											
J_r^π	E_x^{calc} (MeV)	$^{22}\text{Ne}(0_1^+), E_x^{\text{calc}}=0.00$ MeV			$^{22}\text{Ne}(2_1^+), E_x^{\text{calc}}=1.39$ MeV				$^{22}\text{Ne}(4_1^+), E_x^{\text{calc}}=3.42$ MeV				
		$L=0$	$L=2$	$L=4$	$L=0$	$L=2$	$L=4$	$L=6$	$L=0$	$L=2$	$L=4$	$L=6$	$L=8$
0_1^+	0.00	-0.100				-0.607							-0.280
0_2^+	4.02	0.047				0.045							0.058
0_3^+	14.38	0.000				0.001							-0.000
2_1^+	2.00		0.068		-0.055	-0.000	-0.114			0.335	-0.003		0.260
2_2^+	4.03		0.023		0.000	0.012	-0.030			-0.005	0.061		0.009
2_3^+	9.45		-0.081		-0.038	-0.036	0.019			0.026	-0.024		-0.005
2_4^+	10.25		-0.013		-0.003	-0.003	0.006			0.004	-0.004		-0.002
4_1^+	3.52			0.842		-0.334 ^a	0.203 ^a	0.235 ^a	0.239	0.201	-0.263	-0.160	0.135
4_2^+	8.21			0.029		-0.009	0.015	0.015	-0.002	0.001	-0.001	-0.006	0.017

Final states ^{18}O		Initial states						
J_r^π	E_x^{calc} (MeV)	$^{22}\text{Ne}(6_1^+), E_x^{\text{calc}}=6.26$ MeV			$^{22}\text{Ne}(8_1^+), E_x^{\text{calc}}=10.83$ MeV			
		$L=2$	$L=4$	$L=6$	$L=8$	$L=4$	$L=6$	$L=8$
0_1^+	0.00				0.017			0.136
0_2^+	4.02				-0.049			0.041
0_3^+	14.38				0.000			-0.000
2_1^+	2.00		0.551	0.005	0.312		0.509	-0.000
2_2^+	4.03		-0.006	-0.142	0.008		-0.002	0.333
2_3^+	9.45		0.007	0.011	-0.000		0.000	-0.006
2_4^+	10.25		0.004	0.005	-0.000		0.002	-0.001
4_1^+	3.52	-0.227	0.241	0.108	-0.154	0.132	0.054	-0.220
4_2^+	8.21	0.005	-0.000	0.003	-0.002	-0.005	0.001	0.000

^aThe phases of these equivalent spectroscopic amplitudes were inverted in the final calculations.

and/or 4^+ transfer followed by an inelastic scattering); whereas for the population of the 4_1^+ state in ^{18}O the direct one-step transfer should be the major contribution. A judgment of the significance of a certain path is not possible "a priori" in view of the complexity of the mutual influence of individual parameters, but this interdependence is discussed elsewhere.¹⁵

The ZR-coupled channels code CHUCK3 (Ref. 16) has been used for the calculations with the parameters as given in Table I. As in the $(d,^6\text{Li})$ investigation on ^{24}Mg and ^{26}Mg , the finite range correction parameter was kept fixed at 0.57 fm. Figure 7 shows that the ZR-DWBA calculation employing this finite range parameter does not fit the experimental angular distribution as well as the exact FR-DWBA does. However, here we prefer a systematic choice of parameters rather than an individual best fit procedure.

The spectroscopic amplitudes were chosen according to Table III. The deformation parameters β were adjusted according to $\beta_L R$ from scattering results and were chosen from the smaller values of the experimentally deduced variety of numbers:¹⁷⁻²²

$$^{22}\text{Ne}: \beta_2 R = +1.13, \beta_4 R = +0.06,$$

$$^{18}\text{O}: \beta_2 R = +0.82, \beta_4 R = +0.07.$$

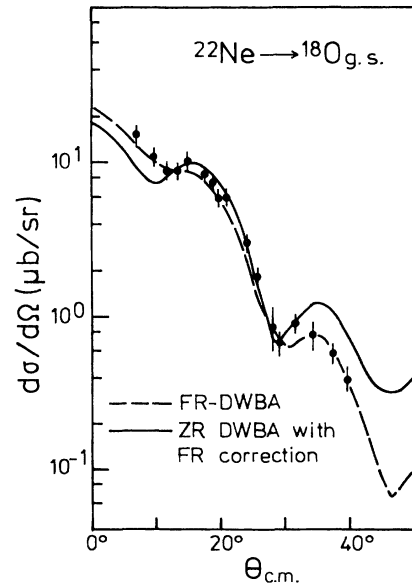


FIG. 7. Comparison of g.s. data with single-step predictions from FR-DWBA (dashed curve) and ZR-DWBA with FR correction (solid curve). Only statistical errors are included in the data.

Results of the calculations are shown in Fig. 8: The one-step paths leading to the final 0^+ , 2^+ , and 4^+ states (dashed lines) and the full CRC case (dashed-dotted lines) with the coupling scheme as shown in Fig. 6. The influence of single paths on the yield of individual final states is shown in Ref. 23, which presents an analysis in the coupled-channels Born approximation (CCBA). The observed disagreement between experimental and theoretical angular distributions for the DWBA case in Fig. 8 is understood in the sense of the FR-DWBA analysis given above; see Table III. Contrary to the CCBA analysis,²³ the CRC calculations seem to be inferior to the DWBA predictions, as the strengths for both the 2^+ and 4^+ states are overpredicted relative to the ground state. Furthermore, especially the small-angle part of the angular distribution for the 4^+ state is in disagreement with the data.

The assumption that the observed failure is due to inconsistencies of spectroscopic phases is supported by the following: (i) even though the spectroscopic *factors* evaluated in the literature for the transitions between ^{22}Ne and ^{18}O [by shell-model calculations using the Chung-Wildenthal interaction³ as well as the Freedom-Wildenthal interaction²⁴ and in the framework of SU(3) (Ref. 10)] agree reasonably well with each other, the predicted *phases* disagree; (ii) an analysis of the $^{24,26}\text{Mg}(d,^6\text{Li})^{20,22}\text{Ne}$ reaction¹⁵ resulted in the need to change the predicted phases; and (iii) an inversion of only the spectroscopic phase for transitions leading from $^{22}\text{Ne}(2^+)$ to $^{18}\text{O}(4^+)$ (see Table III) resulted in very reasonable fits between experimentally observed and CRC-calculated angular distributions. A comparison of these angular distributions is shown in Fig. 9. The discrepancy observed for angles larger than 30° for the ground-state transition is obviously not due to the reaction coupling. The same kind of deviation was observed for the ZR-DWBA calculation (see Fig. 7), indicating that here the ZR-DWBA input parameters were not chosen to be optimum for this particular case. It has been shown²⁵ that, employing different parameter sets, the described discrepancies can be diminished. As an example this is demonstrated by the dashed line in Fig. 9 which is the result of CRC calculations with a 50% increase of the imaginary ^6Li volume potential depth (Table I).

The overprediction of the cross sections for angles

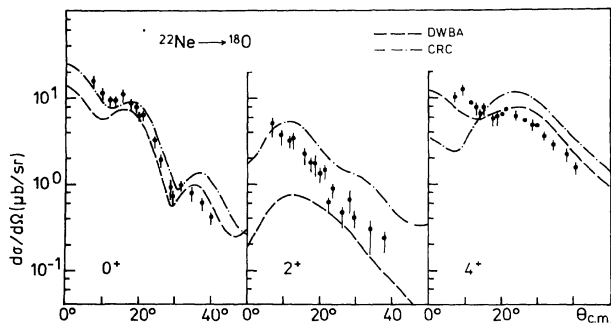


FIG. 8. Data for lowest 0^+ , 2^+ , and 4^+ levels compared with single-step DWBA (dashed) and CRC (dot-dash) calculations. Only statistical errors are included in the data.

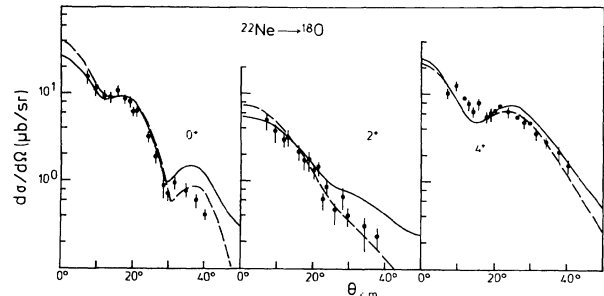


FIG. 9. Data for lowest 0^+ , 2^+ , and 4^+ levels compared with CRC calculations with altered phases (see the text). The solid curves present calculations using the potentials as given in Table I, the dashed curves involve a 50% increase of the imaginary ^6Li volume potential depth. Only statistical errors are included in the data.

larger than 30° of the ground-state transition is obviously propagated to the 2^+ state by the channel coupling. This statement agrees with the influence observed for the individual reaction paths as discussed in Ref. 23. For a discussion of the uncertainties involved in the present type of analysis we refer to an investigation of the $(d,^6\text{Li})$ reaction¹⁵ on magnesium isotopes.

The absolute normalization of the theoretical angular distributions displayed in Figs. 8 and 9 is done such that the full CRC calculation reproduces the magnitude of the experimental cross section for the ground-state transition. Assuming the absolute spectroscopic factor for the “ $d+\alpha=^6\text{Li}$ ” system to be unity and the absolute spectroscopic factors for the ground state transition $^{22}\text{Ne}\rightarrow^{18}\text{O}$ to be correctly predicted by the shell model calculations ($S_\alpha=0.18\times 0.55$, see Ref. 2), the value of the ZR normalization constant D_0 becomes

$$D_0 = 97 \text{ MeV fm}^{3/2}.$$

VI. SUMMARY AND CONCLUSION

The $^{22}\text{Ne}(d,^6\text{Li})^{18}\text{O}$ alpha transfer reaction has been studied at a deuteron energy of $E_d=80$ MeV. Angular distributions were measured and analyzed in the angular range of 8° to 35° laboratory. The FR-DWBA analysis results are in fair agreement with shell-model predictions, indicating that for excitation energies higher than 4 MeV core-excited components are mainly responsible for the observed yields, in agreement with earlier structure studies.¹ The reaction mechanism for populating the lowest 0^+ , 2^+ , and 4^+ states has been investigated using the theory of coupled reaction channel calculations (CRC).

The full CRC treatment results in stronger deviations than observed before in FR-DWBA or in CCBA calculations, especially for the forward angular range of the angular distribution for the 4^+ final state. One possible reason for this difficulty could be due to inconsistencies in phase conventions used in the definition of spectroscopic amplitudes, in deformation parameters, and in the reaction code which are mutually interdependent. A phase change for alpha transitions starting from the initial $^{22}\text{Ne}(2^+)$ state to final states in ^{18}O did result in very

good agreement between experimental angular distributions and CRC calculations for the members of the ground state band, both in shape and in magnitude.

The spectroscopic factors predicted by shell-model calculations prove to be very reliable in the sense that any significant change of one of the individual transition

strengths did worsen and not improve the simultaneous description of the data for the three members of the ground state band in ^{18}O .

We thank Dr. G. Baur and Dr. F. Osterfeld for very helpful discussions.

*Permanent address: Central Research Institute for Physics, Budapest, Hungary.

†Permanent address: Nuclear Physics Division, Bhabha Atomic Research Centre, Bombay 400085, India.

¹R. L. Lawson, F. J. D. Serduke, and H. T. Fortune, *Phys. Rev. C* **14**, 1245 (1976).

²W. Chung, J. van Hienen, B. H. Wildenthal, and C. L. Bennett, *Phys. Lett.* **79B**, 381 (1978); C. L. Bennett, *Nucl. Phys.* **A284**, 301 (1977).

³W. Chung, Ph.D. thesis, Michigan State University, 1976. Shell model calculations, using the computer code of W. Chung.

⁴R. M. DeVries, *Phys. Rev. C* **8**, 951 (1973), finite-range DWBA code LOLA.

⁵W. Oelert, W. Chung, M. Betigeri, A. Djalois, C. Mayer-Böricke, and P. Turek, *Phys. Rev. C* **20**, 459 (1979).

⁶J. D. Childs, W. W. Daehnick, and M. J. Spisak, *Phys. Rev. C* **10**, 217 (1974); W. W. Daehnick, J. D. Childs, and Z. Vreelj, **21**, 2253 (1980).

⁷W. Oelert, G. P. A. Berg, A. Djalois, C. Mayer-Böricke, and P. Turek, *Phys. Rev. C* **28**, 73 (1983), and references therein.

⁸L. T. Chua, F. D. Becchetti, J. Jänecke, and F. L. Milder, *Nucl. Phys.* **A273**, 243 (1976).

⁹P. Lezoch, H. J. Trost, and U. Strohmusch, *Phys. Rev. C* **23**, 2763 (1981).

¹⁰J. P. Draayer, *Nucl. Phys.* **A237**, 157 (1975).

¹¹F. Ajzenberg-Selove, *Nucl. Phys.* **A392**, 1 (1983).

¹²J. Jänecke, E. H. L. Aarts, A. G. Drentje, Y. Iwasaki, R. V. F. Janssens, and L. W. Put, Kernfysisch Versneller Instituut, Groningen, Annual Report, 1980, p. 29.

¹³J. B. A. England, R. Bhowmik, F. D. Brooks, E. C. Pollacco, N. E. Sanderson, and G. C. Morrison, in *Lecture Notes in Physics*, edited by B. A. Robson (Springer, New York, 1978), Vol. 92, p. 470.

¹⁴J. Carter, R. G. Clarkson, V. Hnizdo, R. J. Keddy, D. W. Mingay, F. Osterfeld, and J. P. F. Sellschop, *Nucl. Phys.* **A273**, 523 (1976).

¹⁵W. Oelert, submitted to *Phys. Rev. C*.

¹⁶P. D. Kunz, University of Colorado, code CHUCK (unpublished), modified by J. R. Comfort.

¹⁷H. Rebel, G. W. Schweimer, G. Schatz, J. Specht, R. Löhken, G. Hauser, D. Habs, and H. Klewe-Nebenius, *Nucl. Phys.* **A182**, 145 (1982).

¹⁸J. L. Escudie, R. Lombard, M. Pignanelli, F. Resmini, and A. Tarrats, *Phys. Rev. C* **10**, 1645 (1974); **11**, 639 (1975).

¹⁹B. G. Harvey, J. R. Meriwether, J. Mahoney, A. Bussière de Nercy, and D. J. Horen, *Phys. Rev.* **146**, 712 (1966).

²⁰R. Vandenbosch, W. N. Reisdorf, and P. H. Lau, *Nucl. Phys.* **A230**, 59 (1974).

²¹H. F. Lutz and S. T. Eccles, *Nucl. Phys.* **81**, 423 (1966).

²²J. Stevens, H. T. Lutz, and S. F. Eccles, *Nucl. Phys.* **76**, 129 (1966).

²³W. Oelert and G. Pàlla, in *Proceedings of the 1983 RCNP International Symposium on Light Ion Reaction Mechanism, Osaka, 1983*, edited by H. Ogata, T. Kammuri, and I. Katayama (RCNP, Osaka University, 1983), p. 420.

²⁴M. Conze and D. Manahos, *J. Phys.* **5**, 671 (1979), and references therein.

²⁵W. Oelert and G. Pàlla, Institut für Kernphysik-Kernforschungsanlage Annual Report, 1983.